Available online at www.sciencedirect.com
SCIENCE DIRECT®
Biochemical and Biophysical Research Communications 328 (2005) 251–257
BBRC
www.elsevier.com/locate/ybbrc

Determinants of CD81 dimerization and interaction with hepatitis C virus glycoprotein E2

Heidi E. Drummer*,[1], Kirilee A. Wilson[2], Pantelis Poumbourios[1]

St. Vincent's Institute of Medical Research, 41 Victoria Pde, Fitzroy 3065, Australia

Received 29 November 2004
Available online 6 January 2005

Abstract

The tetraspanin CD81 plays an essential role in diverse cellular processes. CD81 also acts as an entry receptor for HCV through an interaction between the large extracellular loop (LEL) of CD81 and HCV glycoprotein E2. The E2–CD81 interaction also results in immunomodulatory effects in vitro. In this study, we examined the relationship between the dimeric crystal structure of the CD81 LEL and intact CD81. Using random mutagenesis, amino acids were identified that abolished dimerization of recombinant LEL in regions that were important for intermonomer contacts (F150S and V146E), salt bridge formation (K124T), and intramonomer disulfide bonding (T166I, C157S, and C190R). Two monomeric LEL mutants retained the ability to bind E2, K124T, and V146E, whereas F150S, T166I, C157S, and C190R did not. Introduction of K124T, V146E, and F150S mutations in full-length CD81 did not affect its oligomerization and the effects on E2 binding were less severe than for isolated LEL. These results suggest that the LEL has a more robust structure in the intact tetraspanin with regions outside the LEL contributing to CD81 dimerization.

Keywords: CD81; Tetraspanin; Hepatitis C virus; Glycoprotein E2; HCV receptor

CD81 is a tetraspanin present on nearly all nucleated cells and forms multimolecular complexes with a wide variety of cell surface receptors. Tetraspanins contain 4 membrane spanning regions and two extracellular domains that in the case of CD81 are referred to as the small and large extracellular loops (SEL and LEL, respectively). X-ray crystallography of the LEL of CD81 revealed that it is a homodimer with each monomer composed of five α-helices (A–E) arranged in a head subdomain (the last two turns of the A helix, the B, C, and D helices, and their interconnecting loops) atop a stalk subdomain (antiparallel A and E helices) [1]. Four cysteine residues present in all tetraspanins form two intramolecular disulfide bonds that stabilize the head sub-domain while stability of the stalk subdomain is conferred through hydrophobic interactions and two salt bridges between helices A and E [1].

HCV glycoprotein E2 binds with nM affinity to the LEL of CD81. Recently, CD81 and scavenger receptor class B type 1 (SRB-1) have been shown to be essential components of a multireceptor complex used in HCV entry into liver cells [2,3]. In addition, ligation of CD81 by E2 inhibits NK cell activity and lowers the threshold for T cell activation in vitro [4–6], suggesting that E2–CD81 interactions in vivo may play a role in immunomodulation during HCV infection. Recently, we used random mutagenesis of a chimera composed of maltose-binding protein and LEL residues 113–201 (MBP–LEL$^{113–201}$) to determine the amino acids of CD81 that are critical for E2 binding [7]. E2 binding re-

* Corresponding author. Fax: +61 3 9282 2100.
E-mail address: hdrummer@burnet.edu.au (H.E. Drummer).
[1] Present address: Macfarlane Burnet Institute for Medical Research and Public Health Limited, GPO Box 2284, Melbourne Vic 3001 Australia.
[2] Present address: Biochemistry and Cell Biology, Rice University, Houston, TX 77251-1892, USA.

0006-291X/$ - see front matter © 2005 Elsevier Inc. All rights reserved.
doi:10.1016/j.bbrc.2004.12.160

quired solvent exposed hydrophobic residues Ile[182] and Phe[186], Asn[184] that forms part of a hydrophilic pocket adjacent to the Ile[182]–Phe[186] cluster, and Leu[162] that is associated with a nearby hydrophobic cavity. Mutation of these residues in the context of full-length CD81 also abrogated E2 binding confirming their pivotal role in the E2-binding site [7]. Because the three-dimensional structure of the LEL provides a template for computational screening of small molecules with the potential to abrogate the effects of E2–CD81 ligation, it is of vital importance to determine how the structure of the isolated LEL relates to tetraspanin structure.

In this study, random mutagenesis of MBP-LEL$^{113–201}$ was used to identify amino acids critical for LEL dimerization, LEL folding, and E2 binding. Mutations that specifically affected LEL dimerization mapped to residues important for both direct and indirect intermonomer contacts in the LEL dimer. However, these mutations did not always have similar effects when placed in full-length CD81, indicating that the structure of the LEL is more robust in the context of a tetraspanin than in isolation. These studies provide insight into the native CD81 dimer structure and suggest that dimerization is stabilized by regions outside the LEL.

Materials and methods

Expression and purification of MBP-LEL$^{113–201}$. Vector construction, *Escherichia coli* expression, and purification of MBP-LEL$^{113–201}$ have been described [7].

Electrospray mass spectrometry. Electrospray mass spectrometry was performed as described [7,8] on a PE Sciex III+ and nano-electrospray ion source. The ion spectrum was visualized with Tune 2.5-FPU software and deconvoluted using the Hypermass facility in MacSpec 3.3 (Sciex). The redox state of cysteine residues was identified by mass spectrometric analysis of chimeras treated with the alkylating agent 4-vinylpyridine (4-VP; Sigma, 50 mM) [9]. The addition of 105.1 mass units corresponds to the modification of one free sulfhydryl group with 4-VP.

Analytical ultracentrifugation. Purified MBP-LEL$^{113–201}$ oligomer was subjected to sedimentation equilibrium on a Beckman XL-A analytical ultracentrifuge equipped with Absorbance Optics, an An-60Ti rotor, and filled epon centerpieces (12 mm path length). MBP-LEL$^{113–201}$ at 0.5 mg/ml was centrifuged at 10,000 and 18,000 rpm for 16 h at 20 °C. The final equilibrium distributions were determined from absorption measurements at 280 nm. The theoretical partial specific volume calculated from the amino acid composition of MBP-LEL$^{113–201}$ was 0.74 and the solvent density of the buffer was calculated to be 1.013 g/L. To calculate the molecular mass, data were fitted using the SEDEQ1B program to a single species model. The sedimentation coefficient was calculated by sedimentation velocity analysis at 40,000 rpm.

Antibodies. Monoclonal antibody (MAb) to CD81, 1.3.3.22, was purchased from Ancell Immunodiagnostics, Bayport, MN. MAb 9E10, directed to the myc epitope tag, was purified from the cell line MYC 1-9E10.2 using protein G–Sepharose (Amersham–Pharmacia Biotech) according to the manufacturer's instructions and dialyzed into PBS. Monoclonal antibody C8, directed to the HIV-1 gp41 cytoplasmic tail [10], was obtained from the NIAID AIDS Research and Reference Reagent Program. Monoclonal antibodies 9E10 and 1.3.3.22 were radioiodinated by the chloramine T procedure [11] as described previously [12].

Mammalian expression plasmids. The CD81 open reading frame was linked to a C-terminal MAb C8 epitope tag by PCR-amplification using pcDM8-TAPA-1 [13] as template and the primers, 5′-ccg **aagctt**CCACCATGGGAGTGGAGGGCTGC-3′ and 5′-ggc**tctaga** ttatccctcgggcctgtcaggtcccctgggGTACACGGAGCTGTTCCG-3′. The PCR product was cloned into pcDNA3 using *Hin*dIII and *Xba*I to generate pCD81$_{C8}$. The PCR-amplified DNA sequences were verified by automated DNA sequencing. Construction of full-length CD81 mutants was performed using overlap extension PCR from the parent plasmid pCD81$_{C8}$ as described [7].

Cell lines. Human embryonic kidney HEK 293T cells, murine NIH 3T3 cells, and Chinese hamster ovary CHO-K1 cells were maintained in DMEM supplemented with 10% fetal calf serum and 2 mM L-glutamine.

E2^{661} myc production. E2^{661}myc was secreted from HEK 293T cells transfected with pcE2^{661}myc using Fugene 6 (Boehringer–Mannheim) as described [7].

Enzyme-linked immunosorbent assay. The abilities of MBP-LEL$^{113–201}$ chimeras to bind E2^{661}myc were performed using an indirect enzyme-linked immunosorbent assay (ELISA) as described [7].

Random mutagenesis of MBP-LEL$^{113–201}$. Random mutagenesis of CD81 MBP-LEL$^{113–201}$ was performed according to the method of Lin-Goerke et al. [14] as described [7]. Clones that encoded full-length MBP-LEL$^{113–201}$ protein but exhibited reduced E2^{661}myc binding ability were sequenced using big-dye terminator chemistry on a Perkin–Elmer automated sequencer.

Biosynthetic labelling and immunoprecipitation. NIH 3T3 or CHO-K1 cells were seeded in six-well culture plates at 5×10^5 cells/well and transfected 24-h later with plasmid DNA using Fugene 6. At 24-h posttransfection, the cells were labelled with 150 μCi Tran-^{35}S-label (ICN, Costa Mesa, CA) in methionine/cysteine deficient medium for 4 h and then chased in complete medium for a further 18 h. Cell lysates were prepared in lysis buffer (1% Triton X-100, 0.05 M Tris–HCl, pH 7.4, and 0.6 M KCl) and clarified at 10,000*g* for 10 min. Radiolabelled proteins were immunoprecipitated with 7.5 μg of MAb 1.3.3.22 using protein G–Sepharose and separated by SDS–PAGE or semi-native PAGE as described previously [15]. Briefly, for semi-native PAGE, samples were heated to 56 °C for 10 min in sample buffer containing 1% SDS, 5 mM dithiothreitol, 10% glycerol, and 62.5 mM Tris, pH 6.8, and electrophoresed in 10–17% gradient gels lacking SDS. Electrode buffer contained 0.025% SDS. Radioactive proteins were visualized on phosphorimager screens (Molecular Dynamics, Sunnyvale CA).

Western blotting. Western blotting was performed on HEK293T cell lysates using MAb C8 as described [7].

Surface-binding assays. Surface-binding assays were performed using pCD81$_{C8}$ transfected CHO-K1 cells and ^{125}I-labelled MAb 1.3.3.22 to detect surface localized CD81 directly or ^{125}I-labelled MAb 9E10 to detect E2^{661}myc binding to surface localized CD81 as described [7].

Results

Identification of functional determinants in CD81 LEL by random mutagenesis

A random mutagenesis approach was used to identify functional determinants in MBP-LEL$^{113–201}$. Recently, we have reported that MBP-LEL$^{113–201}$ elutes as dimeric and monomeric forms in Superdex 200 gel filtration ([7] and Fig. 1A). Sedimentation equilibrium analysis confirmed the molecular mass of the MBP-LEL$^{113–201}$ putative dimer peak. The experimental data plotted as ($\ln OD_{280}$/radius^2) illustrate a straight line that is consistent with the presence of a stable single solute (Fig. 1B).

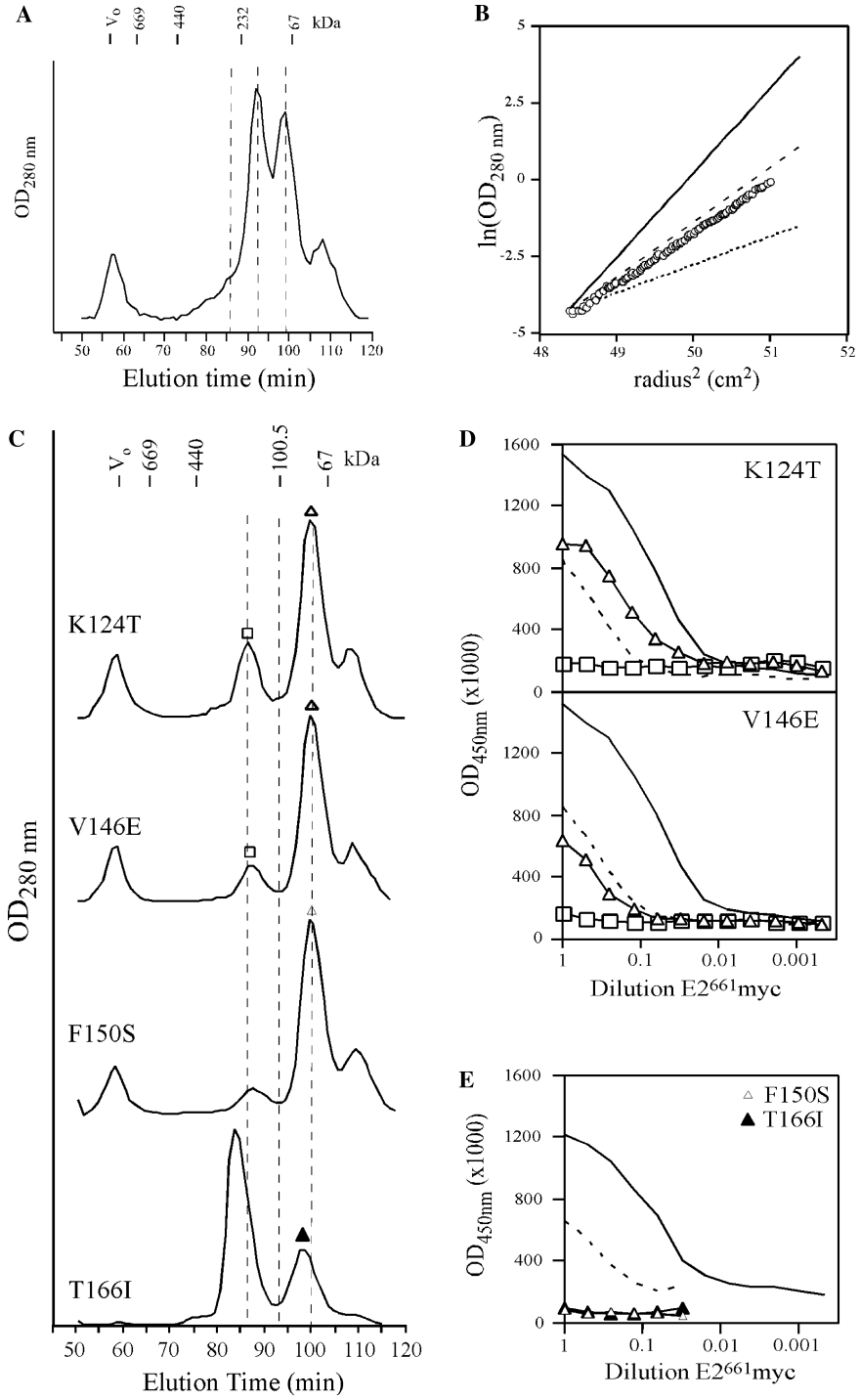

Fig. 1. Separation of wild-type (A) or mutant MBP-LEL$^{113–201}$ (C) oligomeric forms using Superdex 200 gel filtration chromatography. Elution positions for protein standards are indicated above the profiles; the dotted lines indicate the elution positions for putative MBP-LEL monomer (98 min), dimer (92 min), and trimer (86 min). The symbols above gel filtration peaks have been used to identify corresponding MBP-LEL species in (D) and (E). (B) Sedimentation equilibrium of MBP-LEL$^{113–201}$ of 92 min elution peak. Theoretical monomer (dotted line), dimer (dashed line), and trimer (solid line) distributions based on the theoretical molecular weight of monomeric MBP-LEL$^{113–201}$ (50,259 Da). Experimental data, (○). (D,E) Binding of E2^{661}myc to solid-phase wild-type and mutant MBP-LEL oligomeric forms in ELISA. E2^{661}myc-binding was detected with MAb 9E10 and an anti-mouse HRP antibody. For comparison, binding to wild-type dimer (solid line) and monomer (dashed line) are shown.

The slope of the line and the observed molecular mass, 96,300 ± 4,500 Da, closely approximates theoretical dimer mass (100,518 Da). This dimeric form of MBP-LEL$^{113–201}$ exhibited the highest affinity for E2^{661}myc in a competitive ELISA using plate bound MBP-LEL$^{113–201}$ dimer and solution phase oligomers with

an IC_{50} of 30 ± 10 nM compared to 283 ± 29 nM for monomer [7].

Six dimerization incompetent point mutants, K124T, V146E, F150S, C157S, T166I, and C190R, were isolated from the random mutagenesis screen. These mutants eluted in Superdex 200 gel filtration as monomers together with a species eluting in a position corresponding to trimer (Fig. 1C, C157S and C190R are not shown). The $E2^{661}$myc binding abilities of monomeric and oligomeric MBP-$LEL^{113–201}$ were determined initially in ELISA. Fig. 1D shows that K124T and V146E, and wild-type MBP-$LEL^{113–201}$ monomers captured $E2^{661}$myc at similar levels; other oligomeric forms lacked $E2^{661}$myc-binding activity. In solution phase, approximately 3- and 10-fold higher IC_{50}s were observed for K124T (933 ± 58 nm) and V146E (1900 ± 361 nM), respectively, when compared to wild-type. Intramonomer disulfide bond formation was monitored using electrospray mass spectrometry to detect the addition of 4-VP to free sulfhydryl groups (an addition of 105.1 mass units per free sulfhydryl). This technique confirmed that K124T and V146E monomer did not possess free sulfhydryl groups, however, low levels of K124T and V146E dimers were detected (Table 1). The presence of dimers is likely to be due to the formation of hydrophobic aggregates upon storage as analytical gel filtration of K124T and V146E monomers indicated that 5% of the protein had aggregated into a ~400 kDa species (data not shown). These results show that K124T and V146E mutations abolished homodimerization without affecting monomeric LEL folding since intramolecular disulfide bonds had formed and $E2^{661}$myc-binding activity was retained. However, the mutants were less stable than the wild-type monomer possibly accounting for higher IC_{50} values.

In contrast to K124T and V146E proteins, monomeric forms of the remaining four mutants, F150S, C157S, T166I, and C190R, lacked $E2^{661}$myc-binding activity (Fig. 1E and data not shown). Examination of the redox state of C157S, T166I, and C190R monomers by 4-VP/mass spectrometry revealed a free sulfhydryl group for each mutant as well as disulfide-linked dimer (Table 1). These results are consistent with a misfolded LEL moiety that cannot dimerize or bind to E2. Thr^{166} is adjacent to residue Asn^{184} that forms part of the E2-binding site. Although it is likely that this residue is also involved in interaction with E2, it also appears to have a critical role in head subdomain folding. While the F150S mutant also lacked dimerization ability, 4-VP/mass spectrometry analysis indicated the absence of free sulfhydryl groups and disulfide-linked dimer forms (Table 1). This mutant was also the most stable of the monomer mutants with only trace amounts of ~400 kDa aggregate observed in analytical gel filtration after storage for 35 days at 4 °C (data not shown). Phe^{150} is buried in the LEL dimer interface and also participates in the formation of a hydrophobic cluster within each LEL monomer, the LEL-dimerization and E2-binding defects associated with the F150S mutation likely resulting from decreased LEL core hydrophobicity. However, the effects on overall LEL structure appear to be subtle since the monomer is stable and contains two intramolecular disulfide bonds.

Table 1
Mass spectrometry of mutant MBP-LEL chimeras

Mutant species	Expected M_r[a]	Observed M_r[b]
MBP-$LEL^{113–201}$[c]	50,259	50,260
K124T monomer	50,231	50,235, 100,462
V146E monomer	50,288	50,285, 100,576
C190R monomer	50,311	50,427 (1), 100,625
C157S monomer	50,242	50,355 (1), 100,484
F150S monomer	50,198	50,200
T166I monomer	50,270	50,381 (1), 100,540

[a] Daltons.
[b] Free sulfhydryl groups detected by the addition of 105.1 mass units after alkylation with 4 vinyl pyridine to non reduced protein. Number of free sulfhydryl groups indicated in brackets where detected.
[c] Monomeric wild-type MBP-$LEL^{113–201}$.

Mutations in the context of intact cell surface-expressed CD81

To examine the relationship between dimeric LEL crystal structure and intact, cell-surface expressed CD81, we determined whether the K124T, V146E, and F150S mutations that affected MBP-LEL dimerization and/or E2-binding function had analogous effects in the context of the entire tetraspanin. Mutations were introduced into $pCD81_{C8}$, and the expression and stability of the mutants in transfected HEK 293T cells was compared by Western blotting with MAb C8. Fig. 2A indicates the presence of similar amounts of wild-type, K124T, and V146E $CD81_{C8}$ mutants in transfected cell lysates, the proteins migrating as ~26 kDa bands. The F150S $CD81_{C8}$ mutant was present at a lower level with respect to the other constructs perhaps reflecting decreased protein stability.

We compared the ability of wild-type and mutated CD81 molecules to bind secreted $E2^{661}$myc by using a surface-binding assay. We first confirmed the expression of wild-type and mutated $CD81_{C8}$ at the cell surface using radioiodinated anti-CD81 MAb 1.3.3.22. Fig. 2B (inset) shows that ^{125}I-MAb 1.3.3.22 detected similar amounts of wild-type and mutated $CD81_{C8}$ on transfected CHOK1 cells. Using radioiodinated MAb 9E10 we were able to determine whether the mutated $CD81_{C8}$ molecules on the surface of CHOK1 cells bound secreted $E2^{661}$myc. Fig. 2B indicates very similar levels of dose-dependent $E2^{661}$myc-binding to $CD81_{C8}$ and to the K124T mutant while V146E and F150S showed intermediate levels of binding. These data again indicate that mutations affecting isolated LEL dimerization and

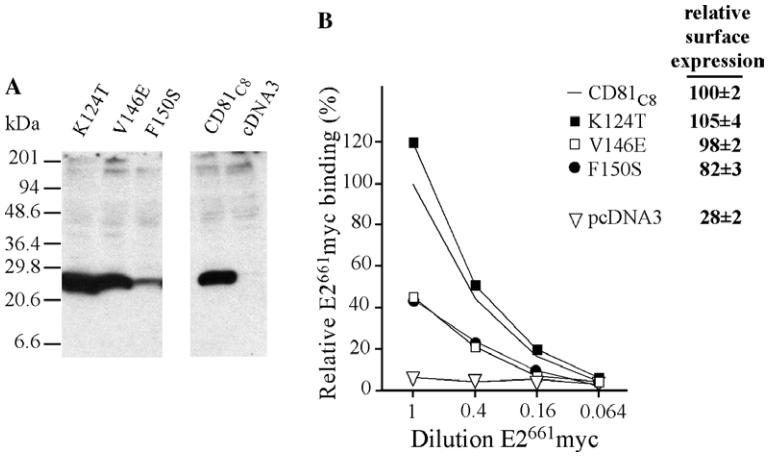

Fig. 2. (A) Synthesis and stability of $CD81_{C8}$ mutants. Lysates of $CD81_{C8}$-expressing 293T cells were subjected to reducing SDS–PAGE in 12–17% polyacrylamide gradient gels, followed by Western blotting with MAb C8, directed to the C-terminal epitope tag. (B) Binding of $E2^{661}$myc to cell surface-expressed $CD81_{C8}$ mutants. Relative $E2^{661}$myc binding is expressed as (ratio of c.p.m. bound to cells expressing mutant $CD81_{C8}$ to c.p.m. bound to cells expressing wild-type $CD81_{C8}$) × 100. The results are representative of two independent transfections. Inset, relative cell surface-expression of $CD81_{C8}$ mutants. Relative [^{125}I]MAb 1.3.3.22 binding to $CD81_{C8}$-expressing cells is expressed as (ratio of c.p.m. bound to cells expressing mutant $CD81_{C8}$ to c.p.m. bound to cells expressing wild-type $CD81_{C8}$) × 100. The means ± SD from three independent transfections are shown.

E2 binding appear to have a less severe effect in the context of the intact tetraspanin.

We next determined if the K124T, V146E, and F150S mutations that blocked MBP-$LEL^{113–201}$ dimerization also affected the oligomeric structure of $CD81_{C8}$ by using a semi-native polyacrylamide gel electrophoresis assay [15]. ^{35}S-labelled $CD81_{C8}$ proteins were extracted from transfected NIH3T3 cells with 1% Triton X-100, shown previously to disrupt heterotypic interactions between CD81 and other cell surface molecules including other tetraspanins [16]. MAb 1.3.3.22-immunoprecipitants were then analyzed under standard reducing SDS–PAGE conditions and semi-native conditions (Figs. 3A and B, respectively). Fig. 3A shows that under standard reducing SDS–PAGE conditions, a ~26 kDa band corresponding to $CD81_{C8}$ could be detected for all constructs, consistent with the expected M_r of CD81. However, under semi-native conditions the appearance of a prominent >36.4 kDa band was observed with a concomitant decrease in ~26 kDa monomer band intensity (Fig. 3B). Standard reducing SDS–PAGE indicated that there were no coimmunoprecipitating ~10 kDa bands present that could potentially give rise to ~36 kDa CD81-containing heterodimers. Recently, similar molecular weights have been observed for monomeric and dimeric CD9 and CD81 tetraspanins [17]. We therefore infer that the ~36.4 kDa band corresponds to CD81 dimer. These results indicate that Lys^{124}, Val^{146}, and Phe^{150} mutations had no detectable effect on CD81 oligomerization, despite their ability to block MBP-$LEL^{113–201}$ dimer formation. The apparent reduction in E2-binding activity observed for V146E and F150S (Fig. 2B) correlates with reduced expression levels compared to K124T and wild-type CD81 (Figs. 2B and 3). The CD81 dimerization domain within the full-length molecule may therefore extend beyond the LEL thereby mitigating the effects of the substitution mutations.

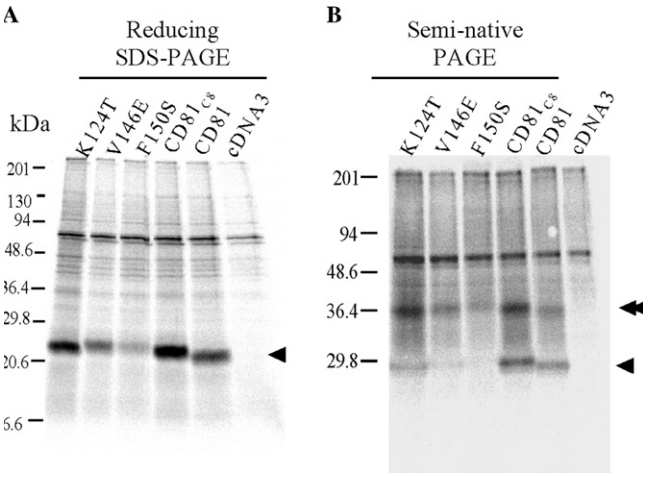

Fig. 3. Oligomerization of $CD81_{C8}$ mutants. Radiolabelled CD81 proteins were immunoprecipitated with MAb 1.3.3.22 and separated by reducing SDS–PAGE (A) or semi-native PAGE (B). Radioactive proteins were visualized on phosphorimager screens. ◀, CD81 monomer; ◀◀, CD81 dimer.

Discussion

In this study, we used MBP–LEL chimeras and random mutagenesis to examine LEL dimerization and binding to HCV E2. The crystal structure of the CD81 LEL (residues 112–202, *h*CD81-LEL) revealed a

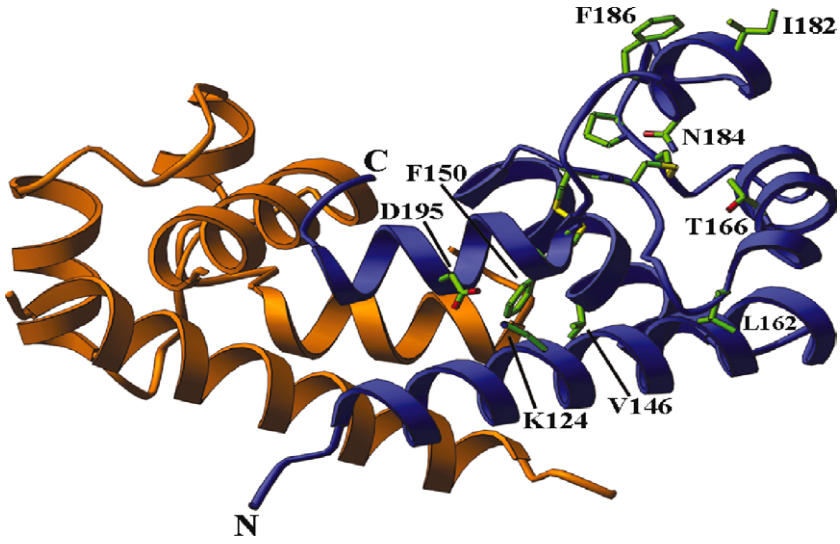

Fig. 4. Ribbon diagram of the *h*CD81-LEL homodimer [1] showing the location of residues identified by random mutagenesis as being important for dimerization (Lys[124], Val[146], and Phe[150]) and E2-binding (Leu[162], Ile[182], Asn[184], and Phe[186]).

homodimer, with each subunit composed of five α-helices (A–E) arranged in a head and stalk subdomain [1]. We show here that MBP-LEL$^{113–201}$ dimerization was blocked by K124T, V146E, and F150S substitutions, consistent with the location of these residues in the *h*CD81-LEL dimer structure (Fig. 4). The hCD81 LEL dimer is stabilized via contacts at the A:A′ helix and B:E′ helix interfaces (the prime indicates the partner monomer) [1]. The A helix residue Lys^{124} forms an intramonomer salt bridge with Asp^{195} of the E helix ([1] and Fig. 4). Ablation of the Lys^{124}–Asp^{195} salt bridge in the isolated LEL may destabilize the antiparallel packing of A and E helices which form the dimerization stalk. The B helix residues Val^{146} and Phe^{150} mediate intermonomer contacts with E′ helix residues Leu$^{197′}$, Phe$^{198′}$, Ser$^{199′}$, and Gly$^{200′}$; the Phe^{150} side chain also participates in the formation of an intramonomer hydrophobic cluster involving Tyr^{127}, Leu^{131}, Val^{147}, and His^{151} [1]. The introduction of polar side chains at these sites would decrease the hydrophobicity of the dimer interface, accounting for the absence of K124T, V146E, and F150S MBP-LEL$^{113–201}$ dimers. K124T and V146E monomers also exhibited decreased stability and E2-binding function relative to their wild-type counterpart while the F150S mutant lacked E2-binding activity altogether. These residues are therefore also important for stabilization of LEL folding (Lys^{124} and Val^{146}) or for attaining the correct conformation for interaction with E2 (Phe^{150}).

By lysing murine 3T3 cells overexpressing CD81 with 1% Triton X-100, a detergent that disrupts tetraspanin–tetraspanin interactions [16], under mildly chaotropic conditions prior to CD81 immunoprecipitation and semi-native SDS–PAGE, we were able to detect a high-order CD81 form within the cell that may correspond to a homodimer. The M_r of this dimeric species was approximately 36.4 kDa, lower than the expected M_r of 52 kDa. Similarly, dimeric CD9 was also observed at a lower M_r than expected [17]. This result suggests that CD81 dimerization is resistant to conditions that normally disrupt tetraspanin–tetraspanin interactions. The stability of this putative CD81 dimer was higher compared to isolated LEL because K124T, V146E, and F150S mutations that blocked MBP-LEL$^{113–201}$ dimerization did not affect CD81 dimerization. The mutations in CD81 described in this study also decreased the E2-binding function of isolated LEL more markedly than for intact CD81 tetraspanin. The relative stability of intact CD81 compared to that of isolated LEL may be due to additional stabilizing intermonomer and intramonomer contacts contributed by regions outside the LEL. For example, the TMDs of tetraspanins appear to have an important function in protein folding and exit from the ER as deletion of the first TMD of CD82 leads to ER retention and prolonged association with the chaperonin calnexin [18]. The SEL of CD81 may also play a role in CD81 biogenesis as modification of this region leads to sub-optimal surface expression [19].

In this study, we confirm that the hydrophobic interface at the A:A′ helix and B:E′ helix interfaces in the LEL crystal structure play a critical role in homodimerization of CD81-LEL monomers. However, our data suggest that additional domains outside the LEL contribute to dimer stability. Such differences between the structures of the isolated LEL and intact CD81 may need to be taken into account in the design of small molecule inhibitors of the CD81–E2 interaction.

Acknowledgments

We thank Anne Maerz for assistance with expression vector construction, and Bruce Kemp for use of the PE Sciex III+ mass spectrometer and the Pharmacia Smart System. This study was supported by Australian National Health and Medical Research Council Project Grants 156714, 205306, and 296200.

References

[1] K. Kitadokoro, D. Bordo, G. Galli, R. Petracca, F. Falugi, S. Abrignani, G. Grandi, M. Bolognesi, CD81 extracellular domain 3D structure: insight into the tetraspanin superfamily structural motifs, EMBO J. 20 (2001) 12–18.

[2] B. Bartosch, A. Vitelli, C. Granier, C. Goujon, J. Dubuisson, S. Pascale, E. Scarselli, R. Cortese, A. Nicosia, F.L. Cosset, Cell entry of hepatitis C virus requires a set of co-receptors that include the CD81 tetraspanin and the SR-B1 scavenger receptor, J. Biol. Chem. 278 (2003) 41624–41630.

[3] J. Zhang, G. Randall, A. Higginbottom, P. Monk, C.M. Rice, J.A. McKeating, CD81 is required for hepatitis C virus glycoprotein-mediated viral infection, J. Virol. 78 (2004) 1448–1455.

[4] A. Wack, E. Soldaini, C. Tseng, S. Nuti, G. Klimpel, S. Abrignani, C. Agrati, C. Nisii, A. Oliva, G. D'Offizi, C. Montesano, L.P. Pucillo, F. Poccia, Binding of the hepatitis C virus envelope protein E2 to CD81 provides a co-stimulatory signal for human T cells, Eur. J. Immunol. 31 (2001) 166–175.

[5] C.T. Tseng, G.R. Klimpel, Binding of the hepatitis C virus envelope protein E2 to CD81 inhibits natural killer cell functions, J. Exp. Med. 195 (2002) 43–49.

[6] S. Crotta, A. Stilla, A. Wack, A. D'Andrea, S. Nuti, U. D'Oro, M. Mosca, F. Filliponi, R.M. Brunetto, F. Bonino, S. Abrignani, N.M. Valiante, Inhibition of natural killer cells through engagement of CD81 by the major hepatitis C virus envelope protein, J. Exp. Med. 195 (2002) 35–41.

[7] H.E. Drummer, K.A. Wilson, P. Poumbourios, Identification of the hepatitis C virus E2 glycoprotein binding site on the large extracellular loop of CD81, J. Virol. 76 (2002) 11143–11147.

[8] M. Wilm, G. Neubauer, M. Mann, Parent ion scans of unseparated peptide mixtures, Anal. Chem. 68 (1996) 527–533.

[9] R.J. Center, B. Kobe, K.A. Wilson, T. Teh, G.J. Howlett, B.E. Kemp, P. Poumbourios, Crystallization of a trimeric human T cell leukemia virus type 1 gp21 ectodomain fragment as a chimera with maltose-binding protein, Protein Sci. 7 (1998) 1612–1619.

[10] Y.H. Abacioglu, T.R. Fouts, J.D. Laman, E. Claassen, S.H. Pincus, J.P. Moore, C.A. Roby, R. Kamin-Lewis, G.K. Lewis, G. Galli, R. Petracca, F. Falugi, S. Abrignani, G. Grandi, M. Bolognesi, Epitope mapping and topology of baculovirus-expressed HIV-1 gp160 determined with a panel of murine monoclonal antibodies, AIDS Res. Hum. Retroviruses 10 (1994) 371–381.

[11] F.C. Greenwood, W.M. Hunter, J.S. Glover, The preparation of I-131-labelled human growth hormone of high specific radioactivity, Biochem. J. 89 (1963) 114–123.

[12] K.A. Wilson, A.L. Maerz, P. Poumbourios, Evidence that the transmembrane domain proximal region of the human T-cell leukemia virus type 1 fusion glycoprotein gp21 has distinct roles in the perfusion and fusion-activated states, J. Biol. Chem. 276 (2001) 49466–49475.

[13] R. Oren, S. Takahashi, C. Doss, R. Levy, S. Levy, TAPA-1, the target of an antiproliferative antibody, defines a new family of transmembrane proteins, Mol. Cell. Biol. 10 (1990) 4007–4015.

[14] J.L. Lin-Goerke, D.J. Robbins, J.D. Burczak, PCR-based random mutagenesis using manganese and reduced dNTP concentration, Biotechniques 23 (1997) 409–412.

[15] P. Poumbourios, D.A. McPhee, B.E. Kemp, Antibody epitopes sensitive to the state of human immunodeficiency virus type 1 gp41 oligomerization map to a putative alpha-helical region, AIDS Res. Hum. Retroviruses 8 (1992) 2055–2062.

[16] S. Charrin, F. Le Naour, M. Oualid, M. Billard, G. Faure, S.M. Hanash, C. Boucheix, E. Rubinstein, The major CD9 and CD81 molecular partner. Identification and characterization of the complexes, J. Biol. Chem. 276 (2001) 14329–14337.

[17] O.V. Kovalenko, X. Yang, T.V. Kolesnikova, M.E. Hemler, Evidence for specific tetraspanin homodimers: inhibition of palmitoylation makes cysteine residues available for cross-linking, Biochem. J. 377 (2004) 407–417.

[18] K.S. Cannon, P. Cresswell, Quality control of transmembrane domain assembly in the tetraspanin CD82, EMBO J. 20 (2001) 2443–2453.

[19] F. Masciopinto, S. Campagnoli, S. Abrignani, Y. Uematsu, P. Pileri, The small extracellular loop of CD81 is necessary for optimal surface expression of the large loop, a putative HCV receptor, Virus Res. 80 (2001) 1–10.